applied sciences

MDPI

Article

Cross-Correlation Frequency-Resolved Optical Gating for Test-Pulse Characterization Using a Self-Diffraction Signal of a Reference Pulse

Yuta Nakano [1,*], Yuichiro Kida [1,2], Kazuya Motoyoshi [1] and Totaro Imasaka [1,3]

1 Department of Applied Chemistry, Graduate School of Engineering, Kyushu University, 744 Motooka, Nishi-ku, Fukuoka 819-0395, Japan; kida@spring8.or.jp (Y.K.); honkichi3@gmail.com (K.M.); imasaka@cstf.kyushu-u.ac.jp (T.I.)

2 RIKEN SPring-8 Center, Koto 1-1-1, Sayo, Hyogo 679-5148, Japan

3 Division of International Strategy, Center of Future Chemistry, Kyushu University, 744 Motooka, Nishi-ku, Fukuoka 819-0395, Japan

* Correspondence: nakano.yuta.048@s.kyushu-u.ac.jp; Tel.: +81-92-802-3295

Academic Editor: Takayoshi Kobayashi

Received: 8 July 2016; Accepted: 19 October 2016; Published: 25 October 2016

Abstract: A diagnostic system using three frequency-resolved optical gating (FROG) techniques—cross-correlation, second harmonic generation, and self-diffraction—is reported for the reliable characterization of femtosecond laser pulses. The latter two FROG techniques are employed to evaluate suitability in measurements of the reference pulse. A train of optical pulses generated by the superposition of two femtosecond pulses emitting at 800 nm and 1180 nm has been characterized by the cross-correlation FROG to evaluate the reliability of the present diagnostic system.

Keywords: ultrafast measurements; ultrafast technology; frequency resolved optical gating

1. Introduction

An ultrashort optical pulse allows the observation of ultrafast phenomena [1,2]. Such a pulse finds a variety of applications, e.g., the ultra-high-precision machining of materials [3] and the sensitive detection of organic compounds in mass spectrometry [4]. Several approaches have been reported to date for their generation. One of the approaches, four-wave Raman mixing in a hydrogen gas, generates octave-spanning multicolor emissions in the optical region [5–7]. By Fourier synthesis of the multicolor emissions, intense sub-2-fs optical pulses can be generated. Ultrashort laser pulses with similar pulse durations have been generated by other schemes, as demonstrated by several groups [8–10]. For the characterization of such extremely short pulses, a diagnostic system covering a wide spectral bandwidth, and hence a sufficiently high time resolution, is required. Available techniques for this purpose include autocorrelation (AC) [11], frequency-resolved optical gating (FROG) [12,13], and spectral phase interferometry for direct electric-field reconstruction (SPIDER) [14,15]. Sub-4-fs pulses have already been characterized by the techniques of spatially encoded arrangement for SPIDER [16] and the dispersion scan (D-scan) [17]. The cross-correlation FROG (XFROG) [18] has been used for the characterization of ultrashort optical pulses as short as 2.4 fs [9]. XFROG is also used in characterizing ultrashort pulses generated by four-wave mixing (FWM) in a bulk medium [19], and ultrashort pulse trains [20]. Recently, methods to extract the information of a carrier envelope phase were reported [21,22]. The phase-matching bandwidth of XFROG is extremely wide, and a few fs optical pulse can be measured when a properly selected nonlinear medium is employed. Note that a low-intensity optical pulse can be characterized using an intense reference pulse in XFROG. In measurements using XFROG, it is necessary to carefully characterize the reference pulse; otherwise, the pulse duration of the test pulse cannot be reliably evaluated.

In this study, an XFROG system is developed for the reliable characterization of ultrashort optical pulses, in which self-diffraction (SD) FROG and second harmonic generation (SHG) FROG are used for the characterization of the reference pulse. In this paper, we report on the combination of SD FROG and XFROG; the reliability of SD FROG was further assured by SHG FROG. This approach is, to our knowledge, the first study in the FROG measurement. Due to the wide spectral domain available, this diagnostic tool would be useful for the measurements of a variety of laser sources emitting in the region extending from the visible to the near-infrared.

2. Experimental Setup

In the experimental setup (Figure 1), a portion of the near-infrared (NIR) optical pulse from a Ti:sapphire regenerative amplifier (35 fs, 800 nm, 4 mJ, 1 kHz, Legend Elite-USP, Coherent Inc., Santa Clara, CA, USA) and a pulse at 1180 nm generated by an optical parametric amplifier (OPA, OPerASolo, Coherent Inc.) pumped by the Ti:sapphire regenerative amplifier were spatially and temporally overlapped to form a two-color femtosecond pulse. This two-color pulse was used as a test pulse while a portion of the NIR pulse from the Ti:sapphire regenerative amplifier (800 nm) was used as a reference pulse for the XFROG measurement.

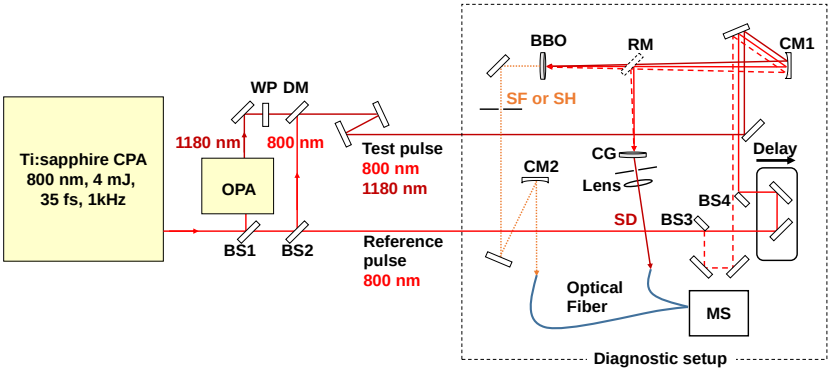

Figure 1. Experimental setup. WP: half-wave plate; DM: dichroic mirror; CM1,2: concave mirror; SF: sum-frequency signal; SH: second harmonic signal; SD: self-diffraction signal; BBO: BBO crystal; RM: removable mirror; MS: multi-channel spectrometer; BS1–4: beam splitter; CG: cover glass.

2.1. Reference Pulse Characterization

Using one of the aluminum-coated D-shaped mirrors (Figure 1, BS3), the reference pulse was split into two parts. One passed through an optical delay line controlled with a closed-loop piezoelectric actuator. These two laser pulses were non-collinearly focused into an SD medium (cover glass, thickness 170 μm) by an aluminum-coated concave mirror (f = 200 mm). The generated SD signal was focused into an optical fiber (QP200-2-VIS-BX, core diameter 200 μm, length 2 m, Ocean Optics, Dunedin, FL, USA) equipped with a multi-channel spectrometer (Maya2000-Pro, Ocean Optics) by a fused-silica lens (f = 50 mm). By scanning the time delay using the piezoelectric actuator, the SD FROG trace was obtained for the reference pulse. A pinhole was used to extract the SD signal. The mirror in front of the SD medium (RM in Figure 1) was then removed to guide the two split pulses into a 5-μm-thick type-I beta-barium borate crystal (BBO, cutting angle $\phi = 90^\circ$ and $\theta = 45^\circ$) to generate the second harmonic of the reference pulse. The distance from RM to the BBO crystal is designed to the same value to that from RM to the SD medium. The silver mirror (RM) has a flat curve for the reflection ratio between 750 nm and 850 nm. For these reasons, the difference in the optical pass is negligible. By focusing the SHG beam into the optical fiber-coupled multi-channel spectrometer using a concave mirror (f = 50 mm) and scanning the time delay using the piezoelectric actuator, the SHG FROG trace was acquired for the reference pulse. A pinhole was used to extract the SHG signal. All the phase

retrievals in the present research were performed using commercial software (FROG3.1.2, FemtoSoft Technologies, 2004, Burlington, MA, USA), and random noise signals were used as initial guesses.

2.2. Test Pulse Characterization

An XFROG trace was obtained using the reference pulse characterized by the above procedure. For this, one of the two replicas of the reference pulse reflected on BS3 (Figure 1) was blocked, and the transmitted beam through the beam splitter was used to gate the test pulse to be characterized. The test pulse consisting of the two-color components was non-collinearly focused into the 5 μm BBO crystal together with one of the replicas of the reference pulse using the concave mirror (CM1 in Figure 1). The angle of the crossing beams was adjusted to be less than ca. 2 degree to avoid geometric smearing. The generated sum-frequency signal between the replica and test pulses was focused onto the multichannel spectrometer to obtain the XFROG trace. The energy ratio between two optical pulses is measured using a power meter (PM10X, Coherent Inc.). This multichannel spectrometer is calibrated to compensate for the change in the spectral response. Phase matching of the SHG and SFG signals using the crystal needs to be considered [23]. Figure 2 shows the phase matching curve calculated by a homemade LabVIEW software (LabVIEW8.6, NATIONAL INSTRUMENTS, 2008, Austin, TX, USA) when using the 800 nm optical pulse as a reference pulse and a 5 μm BBO crystal. A flat phase matching curve is obtained from 800 nm to 1180 nm and from 340 nm to 1500 nm after compensation for a spectral response, supporting a spectral bandwidth allowing a measurement of 1.2 fs optical pulse.

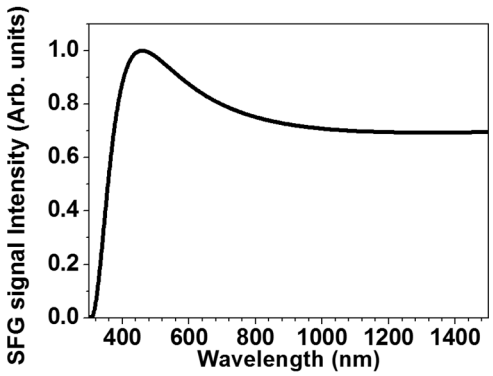

Figure 2. Phase matching curve when a type I 5 μm BBO crystal is used and an 800 nm pulse is used as a reference pulse.

3. Results and Discussion

3.1. Reference Pulse Characterization

The SD and SHG FROG traces measured for the reference pulse are shown in Figure 3a,b, respectively. The SD FROG trace is slightly tilted with respect to a time delay, indicating that the reference pulse was slightly negatively chirped. In contrast, the shape of the SHG FROG trace indicates the presence of the third-order spectral phase distortion [24]. The SHG FROG trace is nearly symmetric; the slight asymmetry is considered to be caused by the slight spatial chirp of the pulses or by the nature of the optics used in this study. To evaluate the reliability in the characterization of the reference pulse, the two temporal intensity profiles of the reference pulse retrieved from the SHG and SD FROG were compared. The FROG errors [13] in the SD FROG and the SHG FROG were 0.4% and 0.5%, respectively, at a grid size of 256 × 256. The small FROG errors suggest that the traces are completely retrieved. In general, two kinds of electric fields are randomly given from a single SHG FROG trace, one of which is the complex conjugated time-reversed replica of the other [13]. One of them was in good agreement with the field retrieved from the SD FROG trace. The temporal intensity profiles (Figure 4a)

retrieved from the SHG and SD FROG traces coincide with each other. The duration of the reference pulse determined by SHG FROG was 58 fs, whereas its duration as characterized by SD FROG was 59 fs; these results are nearly identical. Although the FROG medium and the optical path to the point of measurement are different in these techniques, the temporal phases retrieved from the two FROG traces are in good agreement in the temporal range between −50 fs and 50 fs where 97% of the total energy of the reference pulse is contained. As shown in Figure 4b, the spectral intensity profiles retrieved from the SHG and SD FROG traces are nearly identical to each other. Also, these two FROG analyses converged after 50 to 70 iterations and are reproducible. Note that the SD FROG system allows the characterization of the reference pulse without the ambiguity in the direction of time. On the other hand, it is necessary to check the direction of time by inserting a thin glass plate in the beam path for the SHG FROG measurements [13]. If the time-reversed replica instead of the correct temporal profile was used in the phase retrieval from an XFROG trace, the analysis would lead to a large error in the evaluation of the test pulse [25]. For this reason, SD FROG is preferred for the characterization of a reference pulse. The characterized reference pulse was slightly negatively chirped. A fused-silica plate with a thickness of 19 mm was then placed in the beam path of the reference pulse to minimize the pulse duration. The SD FROG trace measured for the compressed reference pulse (Figure 5a) yields the temporal profile of the reference pulse after phase retrieval (Figure 5b). This compressed reference pulse (43 fs) was then used in the following XFROG measurements. Note that the temporal intensity of the pulse (Figure 5b) is slightly steeper in the trailing edge than the leading edge, which is in contrast to the reference pulse of Figure 4. The feature of the temporal profile would be related to the ratio between the second-order and third-order spectral phases in the pulse. A numerical simulation performed assuming a positive cubic spectral phase in the pulse qualitatively reproduced this temporal behavior. The temporal intensity profile of a laser pulse with a negligibly small second-order phase distortion and a large amount of positive third-order spectral phase distortion is noted to have a steep trailing edge, whereas that with a non-negligible second-order phase distortion and a large positive third-order spectral phase distortion has a steep leading edge.

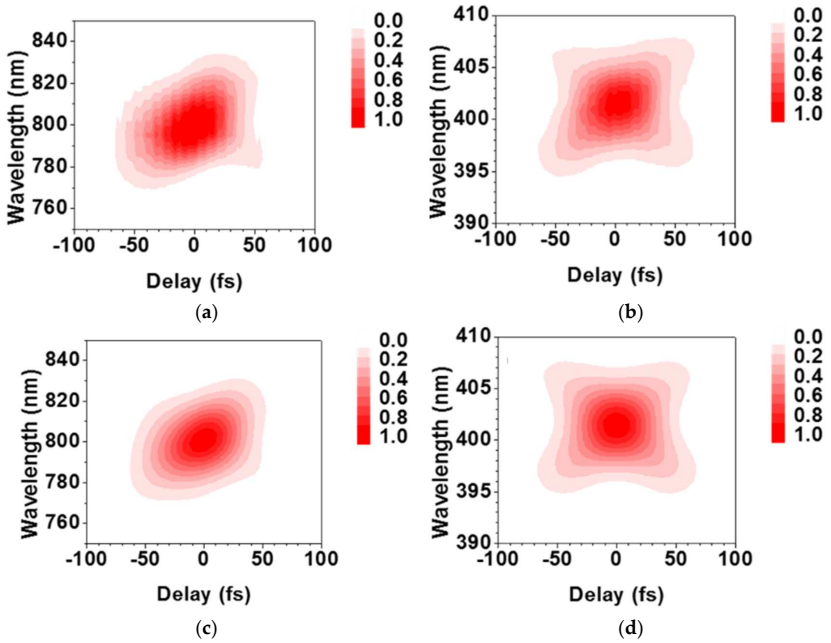

Figure 3. Measured (**a**,**b**) and retrieved (**c**,**d**) SD FROG (**a**,**c**) and SHG FROG (**b**,**d**) traces for the reference pulse.

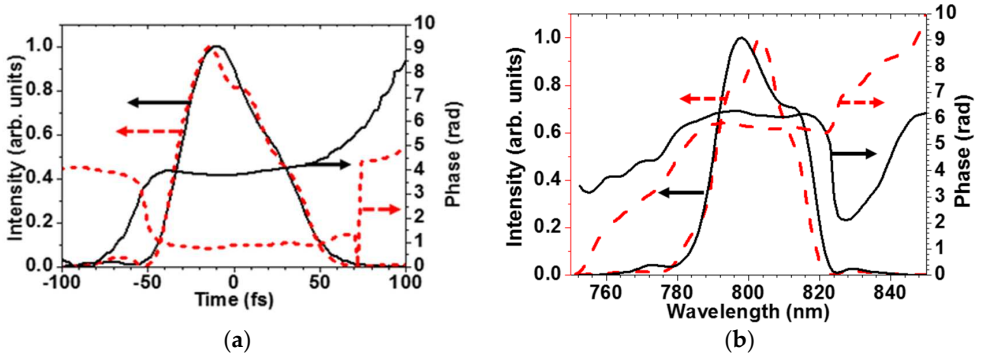

Figure 4. (**a**) Temporal intensity and phase profiles of the reference pulse (800 nm) retrieved from SHG FROG (broken line) and SD FROG (solid line) traces; (**b**) Spectral intensity and phase profiles of the reference pulse.

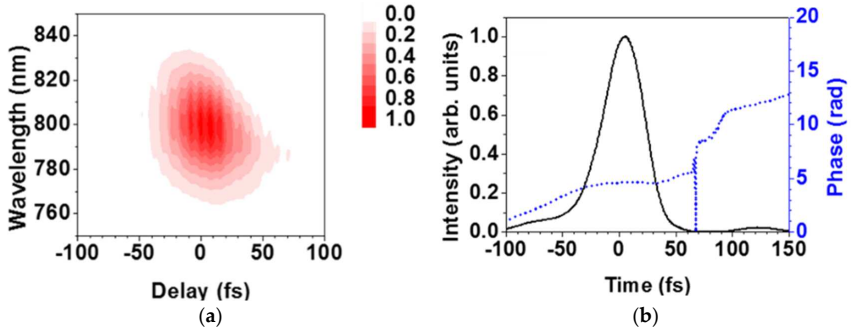

Figure 5. (**a**) SD FROG trace and (**b**) retrieved temporal profile of the reference pulse.

3.2. Test Pulse Characterization

An XFROG trace was measured for the test pulse using the reference pulse shown in Figure 5. The trace consisted of two spectral components (Figure 6a), each of which was generated by the cross-correlation between the reference pulse and one of the two spectral components in the test pulse. The FROG signal measured at 400 nm was generated by sum-frequency mixing between the reference pulse (800 nm) and the pulse at 800 nm contained in the test pulse (hereafter denoted as pulse A). In contrast, the signal at 480 nm was generated by sum-frequency mixing between the reference pulse and the other pulse in the test pulse (1180 nm, hereafter denoted as pulse B).

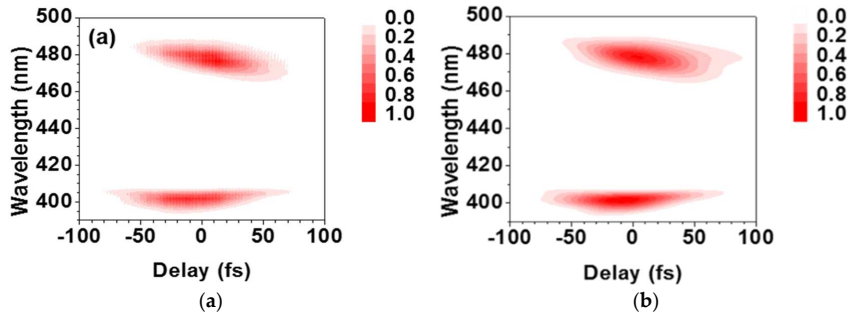

Figure 6. *Cont.*

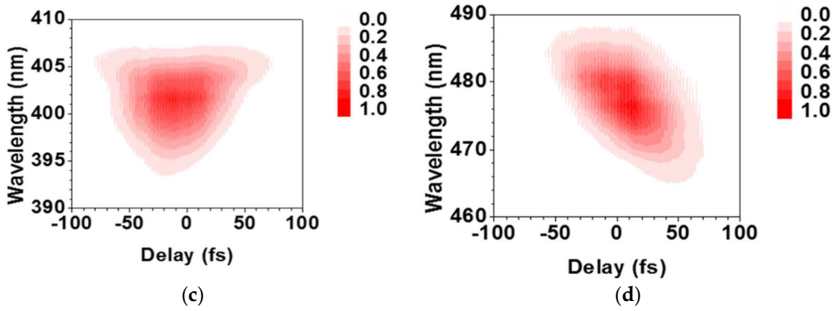

Figure 6. (**a**) Measured XFROG trace; (**b**) Retrieved XFROG trace from (**a**); (**c**,**d**) The expanded views of the cross-correlation signals corresponding to the spectral components at 800 nm and 1180 nm in the test pulse, respectively.

3.2.1. Characterization of Single-Colored Femtosecond Pulses

The temporal profiles of pulses A and B in the test pulse can be retrieved separately by analyzing each of the two FROG signals (Figure 6a). The FROG signal for pulse A (Figure 6c) is symmetric, whereas that for pulse B is tilted with respect to the time delay (Figure 6d). The negative slope of the latter indicates a positive frequency chirp in pulse B. The FROG errors in the analyses of pulses A and B were 0.44% and 0.62%, respectively, yielding the temporal profiles shown in Figure 7. The pulse durations of pulses A and B were calculated to be 51 fs and 55 fs, respectively. To check the reproducibility in the characterization of the pulse, two sets of data were measured independently under the same experimental conditions. In Figure 8, the retrieved temporal intensity profiles obtained from the two XFROG traces are compared. The pulse durations for pulse A (Figure 8a) were 46 fs and 50 fs. Although there is a small difference at the shoulder of the main peak for pulse A, the two temporal profiles are almost identical. The retrieved temporal intensity profiles for pulse B (Figure 8b) suggest pulse durations of 55 fs and 54 fs.

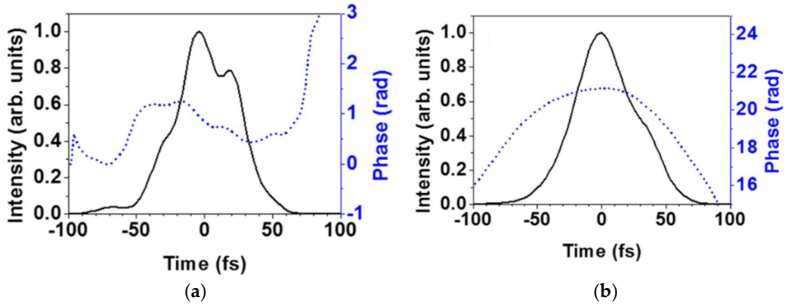

Figure 7. Retrieved temporal intensity (solid line) and phase (broken line) profiles of (**a**) pulse A and (**b**) pulse B.

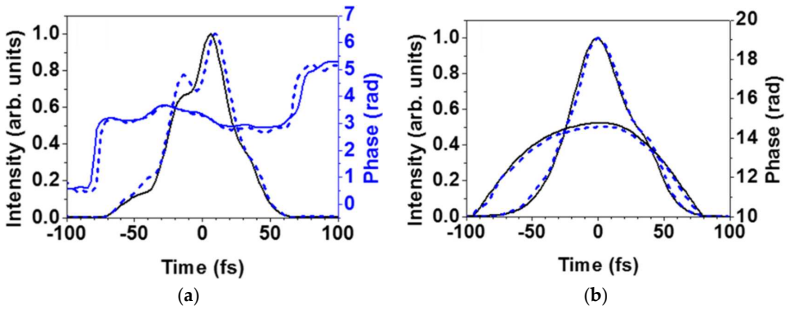

Figure 8. The two sets of retrieved temporal intensities (solid line) and phase (broken line) profiles of (**a**) pulse A and (**b**) pulse B retreived from the two XFROG traces.

3.2.2. Characterization of an Optical Beat

When two color pulses temporally overlap, an optical beat is generated to form a sinusoidal wave with a period determined by the frequency separation. The XFROG trace measured for the test pulse (Figure 6a) indicates that the two femtosecond pulses in the test pulse had temporally overlapped with each other. The temporal intensity profile of an optical beat is determined by the following five parameters: (a) frequency separation; (b) temporal separation; (c) relative intensities at the two frequencies; (d) spectral intensity profile and phase of the two pulses; and (e) relative spectral phase. The four parameters (a–d) are given by the present XFROG measurement. The frequency separation, ca. 4155 cm^{-1}, can be evaluated from the location of the two spectral components. The temporal separation between the two pulses forming the test pulse is evaluated from the relative time delay of the two components in the FROG trace (Figure 6a). The time delays are slightly different from each other, indicating that the two pulses at 800 nm and 1180 nm in the test pulse had not completely overlapped. The relative intensities at the two frequencies are evaluated from the relative intensities of the two signals in the XFROG trace. The spectral intensity profile and the phase of the two pulses are retrieved from the FROG trace as discussed in the previous section. Unfortunately, the relative spectral phase cannot be measured from the FROG trace because of the longer duration of the reference pulse than the spacing of the optical beat. Such a relative spectral phase would provide information of the temporal intensity profile of the optical beat; the envelope of the pulse is determined by the temporal intensity profiles of the two color pulses (Figure 7a,b). This is because the two waves are periodically in phase somewhere within the envelope as long as the width of the envelope is longer than the period of the optical beat. The spacing of the beat is determined by the frequency separation of pulses A and B, not by the relative phase. This would not be the case for an ultrashort optical pulse synthesized using more than two discrete spectral components [26], for instance a pulse train synthesized using multicolor laser emissions generated via FWM [5–7,19]. The characterization of an optical beat formed by two-color laser beams is useful for the evaluation of the bandwidth available in the diagnostics. The accuracy in the relative spectral intensities of the two spectral components retrieved in the FROG analysis allows us to judge whether the diagnostic tool has a broader bandwidth than the frequency separation between the two color pulses or not. The present result suggests that the spectral range is covered from 800 nm to 1180 nm. The FROG error in the phase retrieval was 0.4% at a grid size of 1024×1024. The retrieved XFROG trace (Figure 6b) was in good agreement with the measured XFROG trace (Figure 6a). In the retrieved spectral intensity profile (Figure 9a), there are two spectral components corresponding to pulses A and B. The spectral intensity distribution of the two components agreed well with the shape of the spectral intensity distribution obtained in the phase retrieval, in which the FROG signals of pulses A and B were separately analyzed (see the first paragraph of this section). The ratio of the integrated spectral intensities of these pulses observed in the retrieved spectrum was calculated to be 1.0, which was in good agreement with the energy ratio (0.96) measured using a power meter. This indicates that the relative spectral intensities (Figure 9a) reflect relative intensities of the two pulses. In other words, the bandwidth of the XFROG system was sufficiently broad to support the width corresponding to the frequency separation of the two pulses, i.e., 4155 cm^{-1}. Figure 10 shows the temporal intensity profiles retrieved from two XFROG traces measured independently. As expected from the above discussion, the two temporal intensity profiles of the optical beats are nearly identical to one another: only a slight difference in the relative intensities of the sharp peaks remains. The lack of information about the relative phase thus has given the ambiguity in the relative intensities of the optical beat and in the positions of the sinusoidal wave in the envelope. The other features of the temporal structure of the optical beat, which were determined by the four parameters (a–d), remained in these two measurements. As already discussed above, the two pulses at 800 nm and 1180 nm were not completely overlapping in time. This should result in a change in contrast of the optical beat; the highest contrast was observed in the middle of the temporal profile, while the lowest contrasts were at the leading and trailing edges where the two spectral components do not properly overlap. As mentioned earlier, the spectral component at 1180 nm was

slightly positively chirped, resulting in a decrease in the instantaneous frequency separation between pulses A and B. Thus, the temporal separation of the two adjacent peaks increased at the trailing edge. Accordingly, the temporal structure retrieved from the XFROG trace is determined by the timing and the chirp of the two pulses. It is difficult to characterize a train of pulses with a spectrum consisting of multiple lines by the XFROG because of a lack of information concerning relative phases. However, the temporal waveform of the optical beat consisting of two discrete spectral components is changed only slightly by the change of the relative phase, although the beat is slightly shifted in time. The temporal intensity profile is reported to drastically change with a change in the relative phases among the spectral components when the test pulse consists of more than two discrete spectral components [26]. The present XFROG system would be capable of characterizing such an ultrashort single optical pulse with smooth temporal and spectral profiles even using a long reference pulse [9,27].

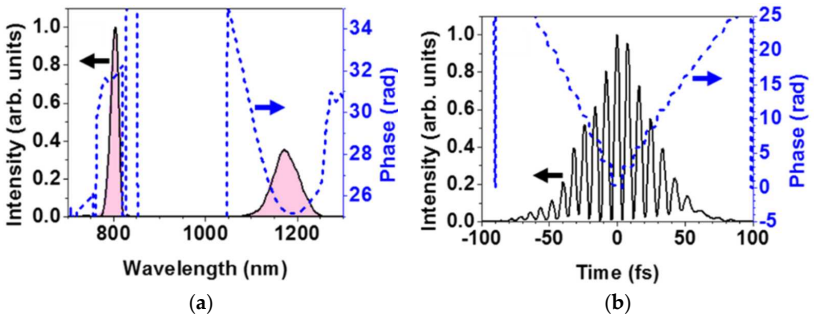

Figure 9. (**a**) Spectral and (**b**) temporal intensity profiles (solid line) and phases (broken line) of the test pulse retrieved from the XFROG trace.

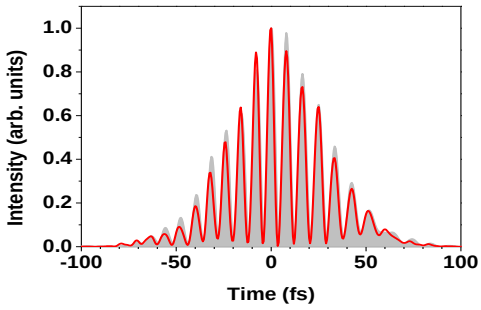

Figure 10. Temporal intensity profiles of the test pulse retrieved from two XFROG traces (solid curve and solid area). One of the two profiles is shifted along the abscissa to match the peak positions of the two profiles for clarity.

4. Conclusions

In summary, we developed a diagnostic tool based on XFROG to reliably characterize ultrashort optical pulses. Using both SHG FROG and SD FROG, it was possible to precisely characterize the reference pulse at the equivalent position where the XFROG signal is generated. This is of crucial importance for characterizing ultrashort pulses based on XFROG. The developed FROG device was applied to the characterization of a test pulse consisting of two femtosecond pulses with different colors. The spectral phases of the two individual pulses were characterized. In addition, the relative spectral intensities of the two pulses were also retrieved. The FROG system developed herein supports a wide spectral range of at least 800–1180 nm. This diagnostic tool can remove the ambiguity of the direction of time for a reference pulse by SD FROG and allows the characterization of the test pulse in an extremely wide spectral region by XFROG. Thus, this approach has a potential for use in the reliable characterization of an ultrashort pulse(s) in the visible and near-infrared regions.

Acknowledgments: This research was supported by a Grant-in-Aid from the Japan Society for the Promotion of Science (JSPS) KAKENHI Grant No. 23245017, No. 24510227, and No. 26220806.

Author Contributions: Performing the experiment: Yuta Nakano, Kazuya Motoyoshi; Data analysis: Yuta Nakano and Yuichiro Kida; Drafting manuscript: Yuta Nakano, Yuichiro Kida; Critical revision, Yuta Nakano, Yuichiro Kida, Totaro Imasaka; Planning and supervision of the research: Yuichiro Kida, Totaro Imasaka.

Conflicts of Interest: The authors declare no conflict of interest.

References

1. Kobayashi, T.; Saito, T.; Ohtani, H. Real-time spectroscopy of transition states in bacteriorhodopsin during retinal isomerization. *Nature* **2001**, *414*, 531–534. [CrossRef] [PubMed]
2. Polli, D.; Altoè, P.; Weingart, O.; Spillane, K.M.; Manzoni, C.; Brida, D.; Tomasello, G.; Orlandi, G.; Kukura, P.; Mathies, R.A.; et al. Conical intersection dynamics of the primary photoisomerization event in vision. *Nature* **2010**, *467*, 440–443. [CrossRef] [PubMed]
3. Kawata, S.; Sun, H.B.; Tanaka, T.; Takada, K. Finer features for functional microdevices. *Nature* **2001**, *412*, 697–698. [CrossRef] [PubMed]
4. Ezoe, R.; Imasaka, T.; Imasaka, T. Determination of triacetone triperoxide using ultraviolet femtosecond multiphoton ionization time-of-flight mass spectrometry. *Anal. Chim. Acta* **2015**, *853*, 508–513. [CrossRef] [PubMed]
5. Sali, E.; Mendham, K.J.; Tisch, J.W.G.; Halfmann, T.; Marangos, J.P. High-order stimulated Raman scattering in a highly transient regime driven by a pair of ultrashort pulses. *Opt. Lett.* **2004**, *29*, 495–497. [CrossRef] [PubMed]
6. Shitamichi, O.; Imasaka, T. High-order Raman sidebands generated from the near-infrared to ultraviolet region by four-wave Raman mixing of hydrogen using an ultrashort two-color pump beam. *Opt. Express* **2012**, *20*, 27959–27965. [CrossRef] [PubMed]
7. Motoyoshi, K.; Kida, Y.; Imasaka, T. High-energy, multicolor femtosecond pulses from the deep ultraviolet to the near infrared generated in a hydrogen-filled gas cell and hollow fiber. *Appl. Sci.* **2014**, *4*, 318–330. [CrossRef]
8. Matsubara, E.; Yamane, K.; Sekikawa, T.; Yamashita, M. Generation of 2.6 fs optical pulses using induced-phase modulation in a gas-filled hollow fiber. *J. Opt. Soc. Am. B* **2007**, *24*, 985–989. [CrossRef]
9. Okamura, K.; Kobayashi, T. Octave-spanning carrier-envelope phase stabilized visible pulse with sub-3-fs pulse duration. *Opt. Lett.* **2011**, *36*, 226–228. [CrossRef] [PubMed]
10. Wirth, A.; Hassan, M.T.; Grguras, I.; Gagnon, J.; Moulet, A.; Luu, T.T.; Pabst, S.; Santra, R.; Alahmed, Z.A.; Azzeer, A.M.; et al. Synthesized light transients. *Science* **2011**, *334*, 195–200. [CrossRef] [PubMed]
11. Diels, J.C.M.; Fontaine, J.J.; McMichael, I.C.; Simoni, F. Control and measurement of ultrashort pulse shapes (in amplitude and phase) with femtosecond accuracy. *Appl. Opt.* **1985**, *24*, 1270–1282. [CrossRef] [PubMed]
12. Kane, D.J.; Trebino, R. Characterization of arbitrary femtosecond pulses using frequency-resolved optical gating. *IEEE J. Quantum Electron.* **1993**, *29*, 571–579. [CrossRef]
13. Trebino, R.; Kane, D.J. Using phase retrieval to measure the intensity and phase of ultrashort pulses: Frequency-resolved optical gating. *J. Opt. Soc. Am. A* **1993**, *10*, 1101–1111. [CrossRef]
14. Iaconis, C.; Walmsley, I.A. Spectral phase interferometry for direct electric-field reconstruction of ultrashort optical pulses. *Opt. Lett.* **1998**, *23*, 792–794. [CrossRef] [PubMed]
15. Iaconis, C.; Walmsley, I.A. Self-referencing spectral interferometry for measuring ultrashort optical pulses. *IEEE J. Quantum Electron.* **1999**, *35*, 501–509. [CrossRef]
16. Witting, T.; Frank, F.; Arrell, C.A.; Okell, W.A.; Marangos, J.P.; Tisch, J.W.G. Characterization of high-intensity sub-4-fs laser pulses using spatially encoded spectral shearing interferometry. *Opt. Lett.* **2011**, *36*, 1680–1682. [CrossRef] [PubMed]
17. Silva, F.; Miranda, M.; Alonso, B.; Rauschenberger, J.; Pervak, V.; Crespo, H. Simultaneous compression, characterization and phase stabilization of GW-level 1.4 cycle VIS-NIR femtosecond pulses using a single dispersion-scan setup. *Opt. Express* **2014**, *22*, 10181–10190. [CrossRef] [PubMed]
18. Linden, S.; Giessen, H.; Kuhl, J. XFROG—A new method for amplitude and phase characterization of weak ultrashort pulses. *Phys. Status Solid B* **1998**, *206*, 119–124. [CrossRef]

19. Weigand, R.; Mendonça, J.T.; Crespo, H.M. Cascaded nondegenerate four-wave-mixing technique for high-power single-cycle pulse synthesis in the visible and ultraviolet ranges. *Phys. Rev. A* **2009**, *79*, 063838. [CrossRef]
20. McCracken, R.A.; Gianani, I.; Wyatt, A.S.; Reid, D.T. Multi-color carrier-envelope-phase stabilization for high-repetition-rate multi-pulse coherent synthesis. *Opt. Lett.* **2015**, *40*, 1208–1211. [CrossRef] [PubMed]
21. Nomura, Y.; Shirai, H.; Fuji, T. Frequency-resolved optical gating capable of carrier-envelope phase determination. *Nat. Commun.* **2013**, *4*, 1–11. [CrossRef]
22. Snedden, E.W.; Walsh, D.A.; Jamison, S.P. Revealing carrier-envelope phase through frequency mixing and interference in frequency resolved optical gating. *Opt. Express* **2015**, *23*, 8507–8518. [CrossRef] [PubMed]
23. Baltuška, A.; Pshenichnikov, M.S.; Wiersma, D.A. Second-harmonic generation frequency-resolved optical gating in the single-cycle regime. *IEEE J. Quantum Electron.* **1999**, *35*, 459–478. [CrossRef]
24. Trebino, R.; DeLong, K.W.; Fittinghoff, D.N.; Sweetser, J.N.; Krumbügel, M.A.; Richman, B.A.; Kane, D.J. Measuring ultrashort laser pulses in the time-frequency domain using frequency-resolved optical gating. *Rev. Sci. Instrum.* **1997**, *68*, 3277–3295. [CrossRef]
25. Kida, Y.; Nakano, Y.; Motoyoshi, K.; Imasaka, T. Frequency-resolved optical gating with two nonlinear optical processes. *Opt. Lett.* **2014**, *39*, 3006–3009. [CrossRef] [PubMed]
26. Kida, Y.; Imasaka, T. Generation of intense subcycle optical pulses in a gas. *Opt. Express* **2015**, *23*, 12373–12381. [CrossRef] [PubMed]
27. Adachi, S.; Kumbhakar, P.; Kobayashi, T. Quasi-monocyclic near-infrared pulses with a stabilized carrier-envelope phase characterized by noncollinear cross-correlation frequency-resolved optical gating. *Opt. Lett.* **2004**, *29*, 1150–1152. [CrossRef] [PubMed]